

Towards Efficient Transferable Preemptive Adversarial Defense

Hanrui Wang*, Ching-Chun Chang, Chun-Shien Lu, and Isao Echizen, *Senior Member, IEEE*,

Abstract—Deep learning technology has brought convenience and advanced developments but has become untrustworthy because of its sensitivity to inconspicuous perturbations (*i.e.*, adversarial attacks). Attackers may utilize this sensitivity to manipulate predictions. To defend against such attacks, we have devised a proactive strategy for “attacking” the medias before it is attacked by the third party, so that when the protected medias are further attacked, the adversarial perturbations are automatically neutralized. This strategy, dubbed *Fast Preemption*, provides an efficient transferable preemptive defense by using different models for labeling inputs and learning crucial features. A forward-backward cascade learning algorithm is used to compute protective perturbations, starting with forward propagation optimization to achieve rapid convergence, followed by iterative backward propagation learning to alleviate overfitting. This strategy offers state-of-the-art transferability and protection across various systems. With the running of only three steps, our Fast Preemption framework outperforms benchmark training-time, test-time, and preemptive adversarial defenses. We have also devised the first to our knowledge effective white-box adaptive reversion attack and demonstrate that the protection added by our defense strategy is irreversible unless the backbone model, algorithm, and settings are fully compromised. This work provides a new direction to developing proactive defenses against adversarial attacks. The proposed methodology will be made available on GitHub.

Index Terms—Transferable preemptive adversarial defense, adaptive reversion attack, proactive defense, adversarial attack.

I. INTRODUCTION

Deep learning technologies have been demonstrated to be sensitive to inconspicuous perturbations (*i.e.*, adversarial attacks) [1]. An adversarial attacker can utilize this weakness to manipulate medias such as images, audios, and videos. For example, the attacker can change the identity of a face image to that of the attacker without changing the looking, enabling the attacker to illegally access (*i.e.*, hack into) the face authentication system [2], [3]. The attacker can also add slight noise on traffic signs, possibly causing an accident during autonomous driving [4]. Defending against such attacks is a critical but unsolved challenge. Passive defenses, on the one

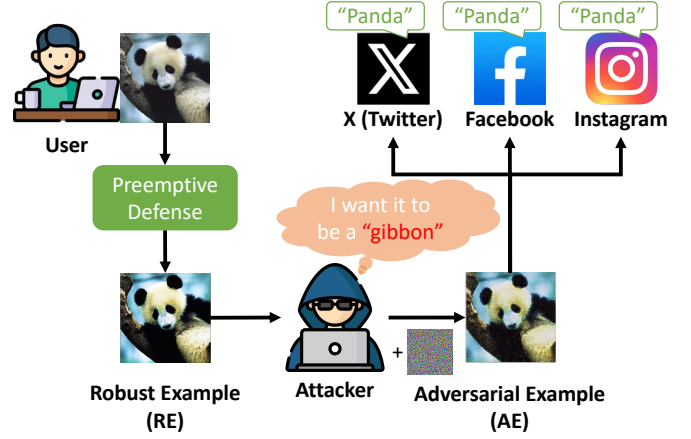


Fig. 1. A preemptive defense offers transferable protection against an adversarial attack by preemptively manipulating the image before it is attacked.

hand, generally sacrifice classification accuracy for resistance against threats [5]–[9]. Proactive defenses, on the other hand, do not achieve satisfactory time efficiency when running protection in real-time applications. Additionally, these proactive defenses typically require paired modules for protection and inference, so their protection is not transferable to other systems [10], [11]. Furthermore, if a provided model is used, the user may concern if backdoor exists in this model [12], [13].

To address these problems, we devise a proactive strategy, called *Fast Preemption*, as illustrated in Figure 1. Fast Preemption preemptively “attacks” (manipulates for enhancement) the medias from the user side before being attacked by the third party. Specifically, Fast Preemption learns robust features and predicts possible adversarial perturbations, then enhances these robust features and reverses the predicted perturbations for purpose of protection. In this case, when these protected medias are further attacked, these adversarial perturbations will be automatically neutralized. This strategy has three distinct advantages. (i) A proactive preemptive defense provides better resistance against threats than a passive one without degrading accuracy, whereas Fast Preemption requires no additional operation for the classification system. (ii) Fast Preemption allows plug-and-play implementation because it does not require paired modules, alleviating the security and privacy concerns through a backdoor when using another provider’s system. (iii) From the attacker’s perspective, once a training- or test-time defense (typically integrated at the classification model) is breached, all inputs are affected. In

Hanrui Wang* (corresponding author), Ching-Chun Chang, and Isao Echizen are with Echizen Lab, National Institute of Informatics (NII), Tokyo, Japan, e-mail: {hanrui_wang, ccchang, iechizen}@nii.ac.jp. Chun-Shien Lu is with Institute of Information Science, Academia Sinica, Taipei, Taiwan. e-mail: lcs@iis.sinica.edu.tw.

This work was partially supported by JSPS KAKENHI Grants JP21H04907 and JP24H00732, by JST CREST Grants JPMJCR18A6 and JPMJCR20D3 including AIP challenge program, by JST AIP Acceleration Grant JPMJCR24U3, by JST K Program Grant JPMJJP24C2 Japan, and by the project for the development and demonstration of countermeasures against disinformation and misinformation on the Internet with the Ministry of Internal Affairs and Communications of Japan.

Manuscript received September 13, 2024.

contrast, with this preemptive defense, only a single user is affected as users are likely to be using different settings. Therefore, Fast Preemption meets four basic requirements:

- *Preserve clean accuracy and improve robust accuracy:* Basic requirements for all defenses.
- *Not require ground truths:* It is impractical to label each input manually.
- *Provide an efficient defense:* Time cost per process must be satisfactory for user interaction.
- *Be transferable to other systems:* Effect of protection must be transferable across various systems, so users do not have to use a paired module.

As illustrated in Figure 2, the Fast Preemption framework includes three components: a classifier model for labeling inputs, a backbone model for learning features, and the forward-backward (*Fore-Back*) cascade learning algorithm for computing protective perturbations. The classifier determines the correctness of the optimization direction. The backbone model greatly determines transferability and time cost. However, the best backbone model must be adversarially trained [5], [14], and its clean accuracy is typically sacrificed for robustness against threats. The Fast Preemption framework uses different models for the classifier and backbone, thereby optimizing both tasks. Additionally, as we demonstrate, the state-of-the-art (SOTA) preemptive defense [10] cannot achieve satisfactory time cost for efficient user interaction. We thus developed the *Fore-Back* cascade learning algorithm combining forward propagation optimization to achieve rapid convergence and backward propagation learning to alleviate overfitting.

We conducted evaluation experiments and ablation studies on two datasets [15], [16] across four models [5]–[8], defending against two typical adversarial attacks [17], [18] in three settings. The results demonstrate the superior performance of the Fast Preemption strategy in terms of clean and robust accuracies, transferability, and time cost compared with those of benchmark training-time, test-time, and preemptive adversarial defenses [7]–[11]. For example, in an end-to-end comparison with the SOTA preemptive defense [10] on the ImageNet dataset [16], Fast Preemption attained 1.5% and 5.6% increases in terms of the clean and robust accuracies, respectively, against AutoAttack (Standard) [18] and was 33 times faster.

Shannon insightfully claimed that “one ought to design systems under the assumption that the enemy will immediately gain full familiarity with them [19].” On the basis of that assumption, we designed the first effective white-box adaptive reversion attack, dubbed *Preemptive Reversion*, for evaluating the reliability of preemptive defenses, *i.e.*, whether they are reversible. As illustrated in Figure 3, Preemptive Reversion conducts the secondary preemptive defense upon the protected example and then reverses these new perturbations because, in the same setting, the secondary defense offers mostly the same perturbations as the first defense. Along with adaptive reversion, we propose using a more comprehensive evaluation protocol, one that requires a decrease in the clean accuracy after the instance is preemptively defended (which is ensured by selecting a poor classifier). If clean accuracy increases

after reversion, the reversion succeeded. If it decreases after reversion (due to distortion), reversion failed.

The results from reversion attack testing demonstrate that the Preemptive Reversion attack can smartly erase protective perturbations when all defense details are compromised (*i.e.*, a white-box situation), whereas blind JPEG distortion and adversarial purification [9] only further distort an image. However, this white-box situation is impractical with the Fast Preemption strategy for real-world applications because the proposed framework enables users to individually customize their defense settings. Apart from a white-box situation, Fast Preemption protection cannot be reversed using existing reversion approaches.

We summarize our contributions as follows:

- We present a new preemptive defense strategy (Fast Preemption) providing more transferable protection without requiring ground truths or requiring users to use a paired module. It is the first to use different models for the classifier and backbone.
- We present a forward-backward (*Fore-Back*) cascade learning algorithm that speeds up preemptive defense for efficient user interaction.
- We present the first effective adaptive reversion attack (Preemptive Reversion) for evaluating the reliability of preemptive defenses in a white-box setting and a more comprehensive protocol to evaluate whether reversion succeeds.

Additionally, we will release a new toolbox upon acceptance that enables plug-and-play implementation with multiple options for each component. This toolbox can also integrate benchmark preemptive defenses.

II. RELATED WORK

Existing adversarial defenses are divided into three categories: training-time, test-time, and preemptive.

Training-time defenses produce robust deep learning models that classify adversarial examples (AEs) correctly. The earliest mechanisms, *e.g.*, adversarial training [1], incorporated various types of AEs along with their ground-truth labels in the training dataset. To improve the efficiency of training on large-scale datasets, Shafahi *et al.* [20] devised accelerated adversarial training in which backward-pass computations are reused. This entails curating a large number of specific real-world samples; Schwag *et al.* [21] circumvented this problem by using additional data from proxy distributions learned by advanced generative models for adversarial training. Goyal *et al.* [5] demonstrated that generative models trained solely on the original dataset can be leveraged to artificially increase the training dataset’s size and improve adversarial robustness against L_p -norm perturbations. Debenedetti *et al.* [6] proposed using a custom recipe of vision transformers for adversarial training in which weaker data augmentation is used with warm-up in the augmentation intensity. Inspired by denoising diffusion models [22], Wang *et al.* [23] conducted adversarial training using data generated by an elucidating diffusion model [24]. Dong *et al.* [25] introduced robust examples (REs) generated by a preemptive defense into the adversarial training

and demonstrated alleviation of clean accuracy deterioration. The current SOTA robust model, devised by Peng *et al.* [7], follows a suite of generalizable robust architectural design principles: (i) an optimal range for depth and width configurations; (ii) a preference for a convolutional rather than patchify stem stage, and (iii) a robust residual block design featuring squeeze and excitation blocks and nonparametric, smooth activation functions.

Training-time defenses have three shortcomings. First, they require vast amounts of data for training, and the data quality and diversity are crucial to robustness. Second, robust models can be counterattacked. Third, training-time defenses typically reduce clean accuracy in favor of robust accuracy, even the one proposed by Dong *et al.* [25], which was designed to circumvent this problem.

Test-time defenses combine detection and purification. Detection models are typically trained on AEs to enable the model to distinguish them from benign inputs. Among recent studies, Cohen *et al.* [26] devised a k-nearest neighbor model for ranking the most supportive training samples for any given validation example in training a detector. Zuo and Zeng [27] proposed using a binary classifier, erase-and-restore, that uses the intriguing sensitivity of L_2 -norm attacks by randomly erasing certain pixels in an L_2 -norm AE and then restoring them with an inpainting technique. Liang *et al.* [28] detected AEs by comparing the classification results of a given sample and a denoised version that was generated through adaptive noise reduction combining scalar quantization and a smoothing spatial filter. Most recently, Hickling *et al.* [29] devised a detector using explainable deep reinforcement learning for uncrewed aerial vehicle agents. However, detection of unseen attacks is challenging for all existing detectors because they are trained on AEs from known attacks. Additionally, detection always introduces errors due to false classification of benign images as AEs, thus reducing clean accuracy.

In contrast, adversarial purification aims to purify AEs by eliminating or invalidating perturbations. Earlier studies used image distortion for purification. For instance, Wang *et al.* [30] distorted images by randomly nullifying pixels. Guo *et al.* [31] preprocessed inputs with a nondifferentiable transformation. Raff *et al.* [32] combined a large number of individually weak defenses into a single randomized transformation to build a strong defense. Lately, more practical approaches generate benign replacements for inputs regardless of whether they are malicious. Ren *et al.* [33] trained a generative model using autoencoder technology [34]. They claimed the existence of an immune space, in which perturbations have fewer adverse effects, and they inactivated adversarial perturbations by restricting them to that subspace. Nie *et al.* [9] devised the DiffPure benchmark, which uses denoising diffusion models [22]. DiffPure replaces perturbations with Gaussian noise and then restores the clean image by reversing the diffusion process. The major limitation of purification is that the difference between the original and generated examples degrades clean accuracy.

Lastly, Alfara *et al.* [35] proposed a test-time defense that integrates the preemptive defense technique as an anti-adversary layer. However, we believe that the use of preemp-

tive defense techniques for test-time defenses is less practical because test-time defenses do not know whether inputs are malicious, so an anti-adversary layer may fail to resist certain attacks because it relies on a label that was predicted from the original classifier and may initially be incorrect.

Preemptive defenses aim to generate REs that replace original images, which are then discarded. These REs are more challenging to manipulate and thus resist adversarial attacks. Salman *et al.* [36] was the first to devise a preemptive defense strategy utilizing REs, which they referred to as “unadversarial” examples. They were learned using projected gradient descent (PGD) [17] and improved both in-distribution performance and robustness against unforeseen perturbations. Moon *et al.* [10] devised a Bi-Level optimization algorithm (abbreviated as Bi-Level in this paper) that finds points in the vicinity of natural images that are robust against adversarial perturbations; it achieved SOTA robust accuracy. However, its time cost is huge, and its transferability is low. Frosio and Kautz [11] introduced the A^5 (“Adversarial Augmentation Against Adversarial Attacks”) framework that uses an individual classifier and a robustifier (a generator), which are co-trained. It is much more efficient than the Bi-Level optimization algorithm, but it is not as robust.

III. PREEMPTIVE DEFENSE STRATEGY: FAST PREEMPTION

With the preemptive defense strategy, the image is preemptively “attacked” (manipulated for enhancement), protecting it before being attacked. In this section, we present the framework and algorithm of our Fast Preemption strategy.

A. Problem Definition

Adversarial attacks and preemptive defenses both manipulate the input by adding subtle perturbations. Specifically, let x and y denote the original image and its ground-truth label, respectively, and let f_v denote the victim model. Let x' denote the manipulated example (AE or RE), formulated as

$$x' = x + \delta, \text{ s.t. } \|\delta\|_p \leq \epsilon, \quad (1)$$

where $\|\cdot\|_p$ represents the L_2 - or L_∞ -norm and ϵ is the setting of the maximum distance. Therefore, adversarial attacks and preemptive defenses aim to solve different optimization problems (as explained below) by changing δ with the inputs of x , y , and f_v .

1) *Adversarial Attack*: An adversarial attack leads to misclassification due to subtle perturbations. Given an original image x and its ground truth y , the adversarial attacker is able to generate an AE by maximizing the cross entropy (CE) loss of x for label y , thereby reducing the model’s confidence in correctly classifying the input as its true label. Therefore, the optimization objective of an adversarial attack for misclassification is

$$\arg \max_{\delta} CE(f_v(x + \delta), y). \quad (2)$$

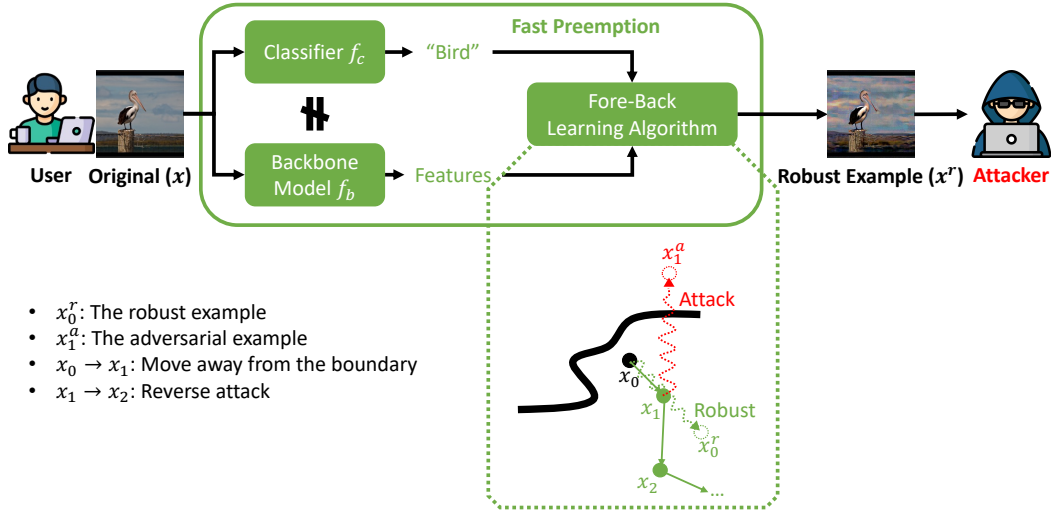


Fig. 2. Fast Preemption framework. The classifier labels inputs automatically, which improves clean accuracy and thereby improves defense performance. The backbone model learns crucial features, so it must be adversarially trained. The Fore-Back learning algorithm first runs forward propagation ($x_0 \rightarrow x_1$) to quickly move away from the incorrect classes and then runs backward propagation ($x_1 \rightarrow x_2$) to alleviate overfitting on the backbone model.

2) *Preemptive Defense*: A preemptive defense aims to generate an RE that will make Equation (2) less successful. Specifically, with the preemptive defense strategy, “backward propagation optimization” is used to reverse the adversarial attack perturbations [10]. In other words, the optimization of Equation (2) remains, but output δ is reversed. The backward propagation optimization is formulated as

$$\arg \max_{\delta} CE(f_v(x - \delta), y). \quad (3)$$

In contrast to backward propagation optimization, we newly define “forward propagation optimization” for the preemptive defense strategy. It directly reverses the optimization direction of Equation (2) from maximization to minimization, which in turn enhances the model’s confidence in accurately classifying the input according to its true label:

$$\arg \min_{\delta} CE(f_v(x + \delta), y). \quad (4)$$

Both the forward and backward optimization learning algorithms will be further addressed in Section III-C.

B. Framework

As illustrated in Figure 2, the Fast Preemption framework includes three components.

Classifier: The correctness of the input labels determines the correct optimization direction for defense. However, for efficient user interaction, it is impractical to label each input manually. Classifier f_c labels these inputs automatically. Therefore, y in Equations (3) and (4) can be replaced by $f_c(x)$. The framework is integrated with user application before being attacked, so f_c does not have to show any transferability or resistance against threats, but it must offer the best classification accuracy. Processing images on the basis of the ground truth can be regarded as using a perfect classifier.

Backbone Model: With Fast Preemption, the input image is iteratively optimized on the basis of feedback from

backbone model f_b , which may differ from victim model f_v in Equations (3) and (4). Therefore, due to its complexity, f_b determines the transferable clean and robust accuracies and time cost. To achieve better performance, the backbone model f_b must be adversarially trained so it can learn more crucial features instead of random pixels. The limitations of adversarially trained models (*i.e.*, training-time defenses), such as the degradation of clean accuracy, are alleviated by the well-performing nonrobust classifier f_c in our framework. As a result, the preemptive defense optimizes the inputs towards the correct labels. Therefore, two different models, classifier f_c and backbone f_b , are integrated into the framework.

Fore-Back Cascade Learning Algorithm: To meet our framework, the optimization problems formulated as Equations (3) and (4) can be reformulated as

$$\arg \max_{\delta} CE(f_b(x - \delta), f_c(x)), \quad (5)$$

$$\arg \min_{\delta} CE(f_b(x + \delta), f_c(x)), \quad (6)$$

respectively, where f_c is our classifier and f_b is our backbone model. This cascade learning algorithm is described in detail in the next section.

C. Forward-Backward (Fore-Back) Cascade Learning Algorithm

The Fore-Back cascade learning algorithm is used to compute protective perturbations. The input is first moved away from the classification boundaries of all incorrect classes so that the manipulated input will be easier to be classified as the ground truth. We define this as *forward propagation* (\rightarrow). Forward propagation can quickly attain convergence (less time cost) but causes overfitting on the backbone model so that the defense is less transferable to other victim models. *Backward propagation* optimization (\leftarrow) is thus conducted following forward propagation. Backward propagation reverses the adversarial perturbations to make them protective perturbations,

which effectively alleviates overfitting and thereby improves transferability. In summary, the forward and backward propagation both enhance robustness, but in different optimization directions.

1) *Loss Function*: From Equations (5) and (6), the loss function of our Fore-Back cascade learning algorithm is the CE loss:

$$\ell(x_i|x, f_c, f_b) = CE(f_b(x_i), f_c(x)), \quad (7)$$

where x_i and x denote the output example of the i -th iteration and the original input, respectively, and f_c and f_b are our classifier and backbone models, respectively. The forward optimization reduces ℓ , while the backward optimization increases it.

2) *Preliminary - Backward Propagation*: The use of backward propagation for preemptive defense was introduced in the SOTA preemptive defense strategy [10]. At each step of that strategy, a PGD attack [17] is run first as $x_1 \rightarrow x_1^a$ (Figure 2), and then the adversarial perturbations are reversed in accordance with the learning rate and thereby forms protective perturbations, as $x_1 \rightarrow x_2$.

Specifically, backward propagation first runs an I -iteration L_∞ -norm PGD attack from x_t , which is the output of the previous optimization step (forward or backward). In other words, the backward propagation increases ℓ via

$$\begin{aligned} x_{t,0} &= x_t, \\ x_{t,i+1} &= \prod_{x,\epsilon} (x_{t,i} + \alpha \cdot \text{sign}(\nabla \ell(x_{t,i}|x, f_c, f_b))), \\ \text{s.t. } \|x_{t,i+1} - x\|_\infty &\leq \epsilon \ \& \ 0 \leq i < I - 1, \end{aligned} \quad (8)$$

where ϵ is the setting of the maximum distance and α is the step size. The final output of Equation (8) is adversarial example x_t^a . Next, backward propagation subtracts perturbations $x_t^a - x_t$ from x_t in accordance with learning rate η , thereby computing the next robust example, x_{t+1} :

$$\begin{aligned} x_{t+1} &= \prod_{x,\epsilon} (x_t - \eta \cdot (x_t^a - x_t)) \\ &= \prod_{x,\epsilon} (x_t - \eta \cdot \alpha \cdot \sum_{i=1}^I \text{sign}(\nabla \ell(x_{t,i}|x, f_c, f_b))). \end{aligned} \quad (9)$$

The SOTA preemptive defense strategy [10] conducts only backward propagation learning. However, adversarial attacks can be randomly initialized, so backward propagation requires many steps to converge (minimum ten steps). The Fast Preemption strategy accelerates defense by running forward propagation before running backward propagation learning.

3) *Combining Forward and Backward Propagation Learning*: We define forward propagation learning as a direct enhancement by moving away from the decision boundary in accordance with the learning rate ($x_0 \rightarrow x_1$ in Figure 2). Therefore, it first reduces ℓ via

$$\begin{aligned} x_{t,0} &= x_t, \\ x_{t,i+1} &= \prod_{x,\epsilon} (x_{t,i} - \alpha \cdot \text{sign}(\nabla \ell(x_{t,i}|x, f_c, f_b))), \\ \text{s.t. } \|x_{t,i+1} - x\|_\infty &\leq \epsilon \ \& \ 0 \leq i < I - 1, \end{aligned} \quad (10)$$

the final output of which is robust example x_t^r . Subsequently, protective perturbations $x_t^r - x_t$ are directly added to x_t in accordance with learning rate η :

$$\begin{aligned} x_{t+1} &= \prod_{x,\epsilon} (x_t + \eta \cdot (x_t^r - x_t)) \\ &= \prod_{x,\epsilon} (x_t - \eta \cdot \alpha \cdot \sum_{i=1}^I \text{sign}(\nabla \ell(x_{t,i}|x, f_c, f_b))), \end{aligned} \quad (11)$$

which is the same as for Equation (9). Therefore, the above derivations can be summarized as

$$\begin{aligned} x_{t,0} &= x_t, \\ x_{t,i+1} &= \begin{cases} \prod_{x,\epsilon} (x_{t,i} - \alpha \cdot \text{sign}(\nabla \ell(x_{t,i}|x, f_c, f_b))) & \rightarrow \\ \prod_{x,\epsilon} (x_{t,i} + \alpha \cdot \text{sign}(\nabla \ell(x_{t,i}|x, f_c, f_b))) & \leftarrow \end{cases} \\ x_{t+1} &= \prod_{x,\epsilon} (x_t - \eta \cdot \alpha \cdot \sum_{i=1}^I \text{sign}(\nabla \ell(x_{t,i}|x, f_c, f_b))), \\ \text{s.t. } \|x_* - x\|_\infty &\leq \epsilon \ \& \ 0 \leq i < I - 1, \end{aligned} \quad (12)$$

where x_* denotes $x_{t,i+1}$ or x_{t+1} . Equation (12) indicates that both forward and backward propagation make the image more robust but with different learning directions for CE loss ℓ .

Whereas backward propagation requires many steps to converge, forward propagation converges quickly. However, forward propagation causes overfitting of the backbone model, so the defense will be less transferable to other victim models. Fast Preemption alleviates this overfitting: T_{\rightarrow} steps of forward propagation are run until there is slight overfitting; then T_{\leftarrow} steps of backward propagation are run to eliminate the overfitting. We evaluated whether the learning is overfitted by evaluating transferability. With this combination of forward and backward propagation, Fast Preemption attains SOTA performance with only three steps (one step T_{\rightarrow} , followed by two steps T_{\leftarrow}), which dramatically reduces the time cost of RE generation.

4) *Averaging N Fast Gradient Sign Method (FGSM) Examples*: Forward and backward propagation both require a backbone optimization algorithm, i.e., an adversarial attack algorithm. For example, The Bi-Level optimization [10] used PGD [17] for backward propagation. However, PGD has to run many sequential iterations to compute superior adversarial perturbations, which greatly increases the time cost. With the Fast Preemption strategy, FGSM [1] is used to speed up the computation of adversarial perturbations.

Since FGSM has difficulty obtaining optimal perturbations, with the Fast Preemption strategy, it is run N times with random initialization to produce N FGSM examples. The perturbations are then averaged to obtain the final output. We demonstrate that averaging the perturbations for PGD examples negligibly affects performance (see Section VII-D), whereas with the Fast Preemption strategy, FGSM optimization is effectively improved while efficiency is preserved.

Furthermore, averaging perturbations in the N FGSM examples is faster than processing a single example with iterative PGD. To generate a single RE, iterative PGD has to run each iteration sequentially from a single input, whereas N FGSM examples can be produced by repeating the single input N

Algorithm 1 Fast Preemption

Input: Original image x , classifier f_c , backbone model f_b , maximum L_∞ -norm distance ϵ , learning rate η , maximum forward steps T_\rightarrow and backward steps T_\leftarrow , number of examples for averaging perturbations N .

Output: Robust example x^r .

```

1: // Forward Propagation
2:  $x_0 = x$ 
3: for  $t < T_\rightarrow$  do
4:   for  $n = 1, \dots, N$  do
5:      $\delta_n \sim U(-\epsilon, +\epsilon)$   $\triangleright$  random initialization
6:      $x_{t,n} = x_t + \delta_n$ 
7:      $x_{t,n}^r = \prod_{x,\epsilon}(x_{t,n} - \epsilon \cdot \text{sign}(\nabla \ell(x_{t,n}|x, f_c, f_b)))$   $\triangleright$ 
       FGSM decreases  $\ell$ 
8:   end for
9:    $\delta_t^r = \frac{1}{N} \sum_{n=1}^N x_{t,n}^r - x_t$   $\triangleright$  averages perturbations
10:   $x_{t+1} = x_t + \eta \cdot \delta_t^r$   $\triangleright$  direct enhancement
11: end for
12: // Backward Propagation
13:  $x_0 = x_{T_\rightarrow}$ 
14: for  $t < T_\leftarrow$  do
15:   for  $n = 1, \dots, N$  do
16:      $\delta_n \sim U(-\epsilon, +\epsilon)$   $\triangleright$  random initialization
17:      $x_{t,n} = x_t + \delta_n$ 
18:      $x_{t,n}^a = \prod_{x,\epsilon}(x_{t,n} + \epsilon \cdot \text{sign}(\nabla \ell(x_{t,n}|x, f_c, f_b)))$   $\triangleright$ 
       FGSM increases  $\ell$ 
19:   end for
20:    $\delta_t^a = \frac{1}{N} \sum_{n=1}^N x_{t,n}^a - x_t$   $\triangleright$  averages perturbations
21:    $x_{t+1} = x_t - \eta \cdot \delta_t^a$   $\triangleright$  reverses the attack
22: end for
23: return  $x^r = x_{T_\leftarrow}$ 

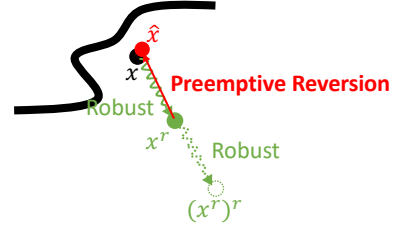
```

times and processing the results in parallel in a single iteration. The improvement attained by averaging the perturbations in N FGSM examples is demonstrated in Table VIII.

5) *Algorithm*: The complete Fast Preemption algorithm is presented in Algorithm 1. With PyTorch implementation, Steps 4 to 8 and Steps 15 to 19 can be respectively processed in parallel.

IV. ADAPTIVE REVERSION ATTACK: PREEMPTIVE REVERSION

A reversion attack is used to evaluate whether a preemptive defense is reversible. In this section, we present the algorithm for our proposed Preemptive Reversion and a more comprehensive protocol for evaluating the effectiveness of reversion attacks. Preemptive Reversion is the only feasible approach to reverse preemptive defense in the white-box scenario. Nevertheless, without full knowledge of the backbone model and settings, our Fast Preemption defense is hard to reverse, so it is reliable.



- $x \rightarrow x^r$: Preemptive defense
- $x^r \rightarrow (x^r)^r$: Preemptive defense in same setting
- $\tilde{x} = x^r - ((x^r)^r - x^r)$: Assume preemptive defenses manipulating similar pixels

Fig. 3. Illustration of Preemptive Reversion algorithm. It first conducts a secondary preemptive defense on RE x^r and then reverses the perturbations of the secondary defense: $(x^r)^r - x^r$.

Algorithm 2 Preemptive Reversion

Input: Robust example x^r .

Output: Reversed example \tilde{x} .

- 1: $(x^r)^r = \text{PreemptiveDefense}(x^r)$ \triangleright secondary defense
- 2: $\tilde{x} = x^r - ((x^r)^r - x^r)$ \triangleright reverses the secondary defense
- 3: **return** \tilde{x}

A. Algorithm

When running preemptive defenses sequentially for the same input and settings, the perturbations are mostly the same for two rounds (see Figure 5). On the basis of this finding, we devised the first effective white-box adaptive reversion attack, i.e., *Preemptive Reversion*, as illustrated in Figure 3. Using RE x^r generated by a preemptive defense method, the Preemptive Reversion algorithm first runs a secondary preemptive defense upon x^r to obtain $(x^r)^r$. Then, the Preemptive Reversion algorithm reverses the secondary perturbations from x^r to obtain \tilde{x} , which is the prediction of the original input x :

$$\tilde{x} = x^r - ((x^r)^r - x^r). \quad (13)$$

The complete algorithm is presented in Algorithm 2.

B. Attack Scenarios

We define two scenarios for a reversion attack in accordance with the knowledge the attacker has about the backbone model and defense algorithm:

- *White-Box*: The attacker knows both the backbone model and defense algorithm (including settings), so the attacker can conduct a secondary defense the same as the user does. This is the strongest, yet impractical, assumption because different users may use different settings.
- *Black-Box*: The attacker knows the defense algorithm (typically public) but not the backbone model (due to infinite selections for users). The major challenge for the attacker in this scenario is that the crucial features learned in the secondary defense may differ from those learned by the user.

Our proposed Preemptive Reversion attack is the first effective reversion attack for evaluating the reversibility of preemptive defenses, including our proposed Fast Preemption defense,

TABLE I
1,000 ORIGINAL CIFAR-10 [15] IMAGES SHOW SIMILAR ACCURACY
WITH THAT OF FULL TEST SET AGAINST AUTOATTACK (STANDARD) [18]
WITH TRAINING-TIME DEFENSE [7] @ $L_\infty \epsilon = 8/255$.

| Number of Test Samples | Clean (%) | Robust (%) |
|------------------------|-----------|------------|
| 10,000 (full) | 93.27 | 71.07 |
| 1,000 (ours) | 93.5 | 71.4 |
| 100 | 95 | 68 |

TABLE II
MODEL ARCHITECTURES.

| Dataset | Architecture |
|----------|-------------------------------------|
| CIFAR-10 | XCiT-L12 [6] |
| | RaWideResNet-70-16 [7] |
| | PreActResNet-18 [5] (backbone) |
| | ResNeXt29-32x4d [37] (classifier) |
| ImageNet | Swin-L [8] |
| | ConvNeXt-L+ConvStem [14] (backbone) |
| | DeiT Base [38] (classifier) |

but it is feasible only in the white-box scenario. Without full knowledge of the defense, Fast Preemption is reliable.

C. Evaluation Protocol

If a reversion attack succeeds, the improved clean accuracy should drop. However, image distortion can create a similar effect. Consequently, a drop in clean accuracy does not necessarily indicate the success of a reversion attack. To address this issue, we proposed a more comprehensive protocol that can distinguish successful reversion from distortion. First, we purposely give incorrect labels to partial inputs to guarantee that the clean accuracy after being defended is lower than the original accuracy. In this situation, if the clean accuracy approaches close to the original accuracy, the reversion attack succeeded. Otherwise, the reversion attack failed, and the deterioration was caused by distortion.

V. EXPERIMENTS

A. Datasets, Classifier, and Backbone Models

We conducted experiments on two datasets: CIFAR-10 [15] (size of 32×32) and ImageNet [16] (cropped to 224×224 to match the requirements of the classifier and backbone model). **CIFAR-10:** We conducted ablation studies using 1,000 samples and then tested our defense and compared the results with benchmarks using another 1,000 samples (resembling the validation and test datasets). ResNeXt29-32x4d [37] and PreActResNet-18 [5] were selected as the classifier and backbone model, respectively. Because Fast Preemption does not require model training, 1,000 samples provided a satisfactory diversity and distribution for testing, as demonstrated by the results listed in Table I. **ImageNet:** We evaluated Fast Preemption and benchmarks using the development dataset from the NIPS 2017 competition, including 1,000 carefully selected ImageNet samples. DeiT Base [38] and ConvNeXt-L+ConvStem [14] were selected as the classifier and backbone model, respectively. The model architectures are listed in Table II.

B. Benchmark Adversarial Defenses

Training-time defenses: We compared Fast Preemption with PreActResNet-18 [5], XCiT-L12 [6], and RaWideResNet-70-16 [7] on the CIFAR-10 dataset. We further compared it with Swin-L [8] on the ImageNet dataset. RaWideResNet-70-16 [7] and Swin-L [8] are the SOTA training-time defenses for each dataset, respectively. As listed in Table II, the model architectures of the SOTA training-time defenses differ from the backbone models, so our experiments are a reasonable way to evaluate transferability.

Test-time defenses: We used DiffPure [9] as the benchmark test-time defense. The inputs (regardless of original or malicious) were purified by DiffPure and then fed into RaWideResNet-70-16 [7] or Swin-L [8] in accordance with the dataset used.

Preemptive defenses. We compared Fast Preemption with two benchmark preemptive defenses: the SOTA preemptive defense, Bi-Level [10], and the latest preemptive defense, A^5 [11]. We used the best defense recipe, “RC (robustifier and classifier),” given by Frosio and Kautz [11].

C. Attacks

Adversarial attacks. We evaluated defenses against two adversarial attacks: PGD [17] and AutoAttack [18]. For AutoAttack, we used both its “Standard” version (combining APGD-CE, APGD-DLR, and FAB [39] and Square Attack [40]) and its “Random” version (combining APGD-CE and APGD-DLR, with expectation over time (EOT) equal to 20 [41]).

Reversion attacks. We ran reversion attacks to evaluate: (i) whether the protected samples induced by preemptive defenses cannot be easily and precisely reversed back to their original unprotected status, which we define as “irreversible” in this paper; (ii) whether the proposed adaptive reversion attack, Preemptive Reversion, is effective. Therefore, apart from the specific Preemptive Reversion, we also ran reversion attacks using blind distortion (JPEG compression) and adversarial purification (DiffPure [9]).

D. Evaluation metrics

We used both clean accuracy and robust accuracy for performance evaluation, where higher accuracy is better from the defense perspective. Here, accuracy refers to the ratio of predictions that match their ground-truth labels. Clean accuracy was computed for benign images (original and REs) while the robust accuracy was computed for AEs. Additionally, to capture the image quality, the structural similarity index measure (SSIM) [42] was computed with respect to the original images. A larger SSIM indicates a more subtle change.

E. Implementation

Our implementation partially leveraged the ART [43] and RobustBench [44] leaderboards by using PyTorch. The experimental machine was equipped with an NVIDIA A100 40GB GPU.

TABLE III
EXPERIMENT SETTINGS.

| Type | Approach | Settings |
|--------------------|------------|--|
| Adversarial Attack | PGD | $L_\infty \epsilon = \frac{8}{255} / \frac{4}{255}^2$ or $L_2 \epsilon = 0.5^1 / 2^2$ |
| | AutoAttack | |
| Reversion Attack | JPEG | Quality Factor = 50% |
| | DiffPure | Diffusion Timestep = $0.1^1 / 0.15^2$ |
| | Ours | Same with our defense |
| Defense | DiffPure | Diffusion Timestep = $0.1^1 / 0.15^2$ |
| | Bi-Level | $L_\infty \epsilon = \frac{8}{255} / \frac{4}{255}^2$ $\eta^3 = 0.1, T_{\leftarrow} = 100, N = 1$ |
| | A^5 | $L_\infty \epsilon = \frac{8}{255} / \frac{4}{255}^2$ |
| | Ours | $L_\infty \epsilon = \frac{8}{255} / \frac{4}{255}^2$ $\eta^3 = 0.7, T_{\rightarrow} = 1, T_{\leftarrow} = 2, N = 20$ |

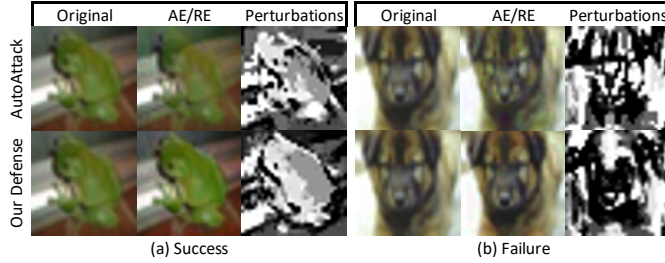
¹ for CIFAR-10; ² for ImageNet.³ η must meet $\eta \cdot (T_{\rightarrow} + T_{\leftarrow}) > 1$.

Fig. 4. Perturbations of adversarial attacks and proposed preemptive defenses. Observation of differences between original image and RE show that Fast Preemption perturbations are unnoticeable. Comparison of perturbations between AutoAttack and Fast Preemption show that preemptive defense is more likely to succeed when perturbations are similar.

VI. PERFORMANCE

In this section, we present the end-to-end evaluation results and comparisons with benchmarks. The results were obtained in the settings listed in Table III.

A. Robustness against Adversarial Attacks

We evaluated transferable defense performance for the situation in which the defense has no knowledge of the AutoAttack [18] and victim models [7], [8]. Table IV compares the performance of Fast Preemption with that of the benchmark defenses against AutoAttack [18]. Fast Preemption performance was better than that of the benchmarks in terms of clean and robust accuracies, whereas its time cost was competitive. For example, in comparison with the least time costly method RaWideResNet-70-16 [7] with the CIFAR-10 dataset, Fast Preemption had 2% and 12.8% better clean and robust accuracies (Standard L_∞), respectively, with 0.04 more seconds per generation. Compared with the SOTA preemptive defense, Bi-Level [10], which had the second best accuracy, Fast Preemption had 3.3% and 5.5% better clean and robust accuracies (Standard L_∞), respectively and was 700 times faster. Note that preemptive defenses can work together with training-time and test-time defenses. For example, when combined with a test-time defense, the performance of Fast Preemption was remarkably improved, as reflected in the last row of Table IV.

Figure 4 illustrates the results of qualitative analysis. A visual comparison of the original image and RE (average

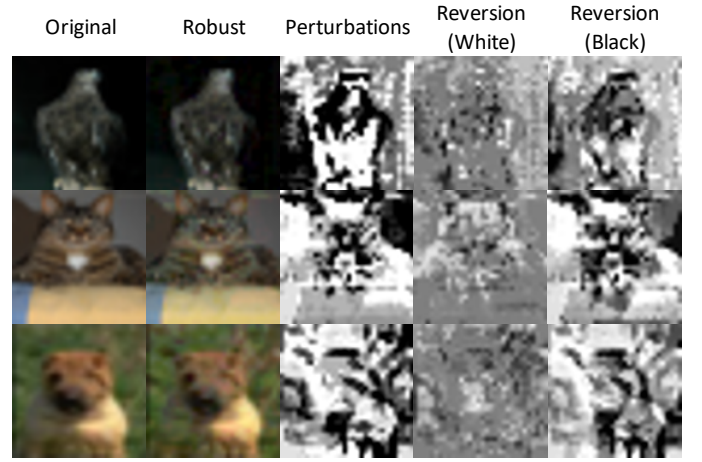


Fig. 5. Perturbations before and after proposed Preemptive Reversion attack. White-box reversion successfully erased most protective perturbations while black-box reversion failed.

SSIM 0.962) revealed that the perturbations generated by Fast Preemption are unnoticeable. Moreover, the “Success” and “Failure” cases indicate that preemptive defense is more likely to succeed when the perturbations are similar to the attack ones. Note that the perturbation illustration δ_{Gray} was drawn by first normalizing the true perturbations δ from $[-\epsilon, +\epsilon]$ to $[0, 1]$ to produce δ_{RGB} and then transforming δ_{RGB} into grayscale using the National Television Standards Committee (NTSC) formula [45]:

$$\begin{aligned} \delta_{RGB} &= \frac{\delta + \epsilon}{2 \cdot \epsilon}, \\ \delta_{Gray} &= 0.299 \cdot \delta_{RGB}.R + \\ &\quad 0.587 \cdot \delta_{RGB}.G + 0.114 \cdot \delta_{RGB}.B, \end{aligned} \quad (14)$$

where $\delta_{RGB}.R$, $\delta_{RGB}.G$, and $\delta_{RGB}.B$ represent the red, green, and blue channels, respectively.

B. Resistance against Reversion Attacks

We conducted reversion attacks to evaluate whether preemptive defenses are reversible. Apart from the proposed Preemptive Reversion attack, we used JPEG compression and adversarial purification because they require no knowledge of the defense. Preemptive Reversion was evaluated in both white- and black-box scenarios (see Section IV-B). The results are summarized in Table V. The results shown in red approach the original accuracy, demonstrating that only our reversion attack was able to reverse the preemptive defense. The other reversion attacks failed because they further reduced clean accuracy (due to distortion). Nevertheless, Preemptive Reversion is only feasible in the white-box setting. Without full knowledge of the defense, Fast Preemption is irreversible. Figure 5 further supports our claim that the white-box reversion successfully erases most protective perturbations while the black-box reversion fails. However, the white-box reversion cannot fully remove the protective perturbations due to the randomization in Fast Preemption (*i.e.*, randomly initialized FGSM).

TABLE IV
END-TO-END PERFORMANCE AGAINST AUTOATTACK [18] AND COMPARISON WITH BENCHMARK ADVERSARIAL DEFENSES.

| Dataset | Defense | | Time Cost (s) | Clean (%) | Standard L_∞ (%) | Standard L_2 (%) | Random L_∞ (%) |
|----------|---------------------------------------|------------------------|---------------|-------------|-------------------------|--------------------|-----------------------|
| CIFAR-10 | Training-Time | RaWideResNet-70-16 [7] | 0 | 93.3 | 72.8 | 69.3 | 73.4 |
| | Test-Time | DiffPure [9] | 0.3 | 91.4 | 75.8 | 83.7 | 76.2 |
| | Preemptive | A^\flat [11] | 0.01 | 93.2 | 72.4 | 68.1 | 73.0 |
| | | Bi-Level [10] | 28 | 92.0 | 80.1 | 78.0 | 80.2 |
| | | Fast Preemption (ours) | 0.04 | 95.3 | 85.6 | 84.5 | 85.7 |
| ImageNet | Training-Time | Swin-L [8] | 0 | 93.0 | 67.0 | 59.5 | 67.5 |
| | Test-Time | DiffPure [9] | 1.2 | 88.8 | 73.7 | 79.4 | 73.8 |
| | Preemptive | Bi-Level [10] | 43 | 93.6 | 71.5 | 62.8 | 72.3 |
| | | Fast Preemption (ours) | 1.3 | 95.1 | 77.1 | 67.4 | 78 |
| | Fast Preemption (ours) + DiffPure [9] | | 2.5 | 93.3 | 82.9 | 87.6 | 83.4 |

TABLE V
PREEMPTIVE DEFENSES RESIST REVERSION ATTACKS.

| Original (%) | Preemptive Defense | | | Clean (%) | Distortion JPEG (%) | Purification DiffPure (%) | Preemptive Reversion (ours) | |
|--------------|--------------------|-----------------|----------|-----------|---------------------|---------------------------|-----------------------------|-----------|
| | Classifier | Backbone | Approach | | | | White (%) | Black (%) |
| 93.5 | Bi-Level | Bi-Level | Bi-Level | 91.9 | 90.5 | 90.8 | 93.1 | 90.7 |
| | Bi-Level | PreActResNet-18 | Bi-Level | 91.2 | 90.6 | 90.7 | 93.4 | 91.0 |
| | Bi-Level | PreActResNet-18 | Ours | 91.3 | 90.5 | 90.5 | 93.4 | 90.6 |
| | ResNeXt29-32x4d | PreActResNet-18 | Ours | 95.5 | 94.4 | 94.8 | 94.0 | 94.6 |

Numbers in red demonstrate that only our reversion attack is feasible but only in the white-box setting.

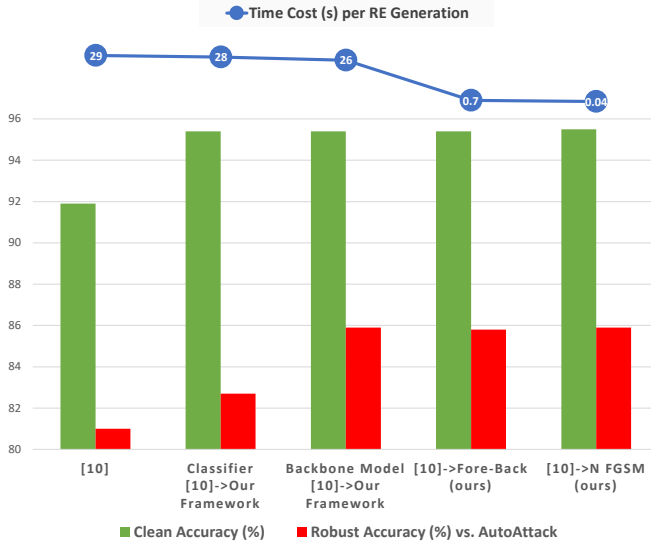


Fig. 6. Compared with the SOTA preemptive defense Bi-Level [10], our framework improved the clean and robust accuracies, and our learning algorithm reduced the time cost for defense.

Moreover, the results in the fourth row of Table V, which were obtained without using our evaluation protocol, demonstrate that our protocol for evaluating reversion attacks is more comprehensive. The results shown in the other rows demonstrate that our Preemptive Reversion in the white-box setting is the only feasible reversion attack as it is the only one for which clean accuracy was higher after reversion. However, the lower numbers in the fourth row indicate that the decrease in accuracy with Preemptive Reversion in the white-box setting was due to successful reversion, whereas the other decreases were due to distortion. Therefore, if only the results in the fourth row are considered, a decrease in accuracy does not necessarily indicate the effectiveness of a reversion attack.

TABLE VI
PERFORMANCE WITH DIFFERENT CLASSIFIERS.

| Ablation Classifier | Accuracy(%) | Time Cost(s) | Transferable Defense | | |
|---------------------|-------------|--------------|----------------------|-------------|---------------|
| | | | Clean(%) | PGD(%) | AutoAttack(%) |
| Ground Truths | 100 | 28 | 97.2 | 86.9 | 83.1 |
| ResNeXt | 95.9 | 28 | 95.4 | 85.7 | 82.7 |
| Bi-Level | 89.1 | 29 | 91.9 | 83.9 | 81.0 |

To evaluate the performance of diverse classifiers in our framework, we used the same backbone model and 100 steps backward propagation as Bi-Level [10]. The transferable defenses were all evaluated using RaWideResNet-70-16 [7] as the victim model.

VII. ABLATION STUDIES

We conducted ablation studies on the Fast Preemption framework and learning algorithm using the CIFAR-10 dataset. The attacks were PGD [17] and AutoAttack (Standard) [18] with L_∞ -norm perturbations and $\epsilon = 8/255$. As illustrated in Figure 6, Fast Preemption with the proposed framework and learning algorithm outperformed the SOTA benchmark Bi-Level [10] in terms of clean and robust accuracies and time cost. These studies and results were aimed at identifying the optimal strategies.

A. Classifier

In all proactive defenses, correct labeling guarantees that optimization moves in the correct direction. As demonstrated in Table VI, a classifier with higher accuracy leads to better performance. As this classifier is not involved in the Fore-Back learning, the time cost of labeling inputs can be ignored compared with that of Fore-Back learning. Note that the use of ground truths is ideal, but this requires manual labeling, which is impractical for efficient user interaction. Therefore, we used the best pretrained classifier in the Fast Preemption framework, one that differs from the backbone model.

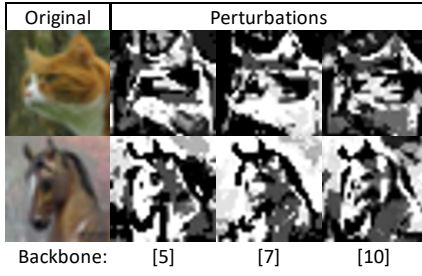


Fig. 7. Different backbone models learn different features. PreActResNet-18 [5], RaWideResNet-70-16 [7], and Bi-Level [10] were adversarially trained, so they learned more crucial features, *i.e.*, ones that are visually similar to the objective.

B. Backbone Model

The backbone model determines the defense time cost and performance. As illustrated in Figure 7, different backbone models learn different features. To evaluate the effect of the backbone model, we also evaluated white-box defenses, for which the backbone model is the same as the victim model, *i.e.*, paired modules, as stated in Section I, although we believe that this setting is not secure due to potential privacy leakage due to the existence of a backdoor [13].

As shown in Table VII, the best adversarially trained model was RaWideResNet-70-16 [7], so it is not surprising that its white-box defense outperformed that of the other backbone models. However, this most robust model failed to guarantee the best transferability, and the time cost was much higher due to its complexity. We thus empirically selected PreActResNet-18 [5] as the backbone model in Fast Preemption as it had the least time cost and best transferability. Nevertheless, it is worth investigating more comprehensive approaches for determining the backbone model in future work.

C. Forward-Backward (Fore-Back) Cascade Learning

As observed in Figure 8, forward (F) propagation accelerated defense but led to overfitting (*e.g.*, F100-B0). In contrast, backward (B) propagation required more steps to converge (*e.g.*, F0-B100) but alleviated overfitting by the forward propagation (*e.g.*, F10-B90). Additionally, as shown by the curve for “Alternate,” the number of steps in forward propagation must be smaller than that in backward propagation to alleviate overfitting.

Our goal is to reduce the time cost, *i.e.*, learning steps, so we further evaluated forward and backward propagation by limiting the learning steps, as illustrated in Figure 9. The results show that when the number of learning steps is small, the combination of forward and backward propagation outperforms backward propagation alone (*e.g.*, F1-B2 vs. F0-B3). Therefore, Fast Preemption runs one step forward and two steps backward propagation learning as the optimal strategy.

D. Optimization Algorithm

The results in Table VIII indicate that averaging N FGSM examples results in the best performance with the least time cost. Using PGD results in much more time being spent

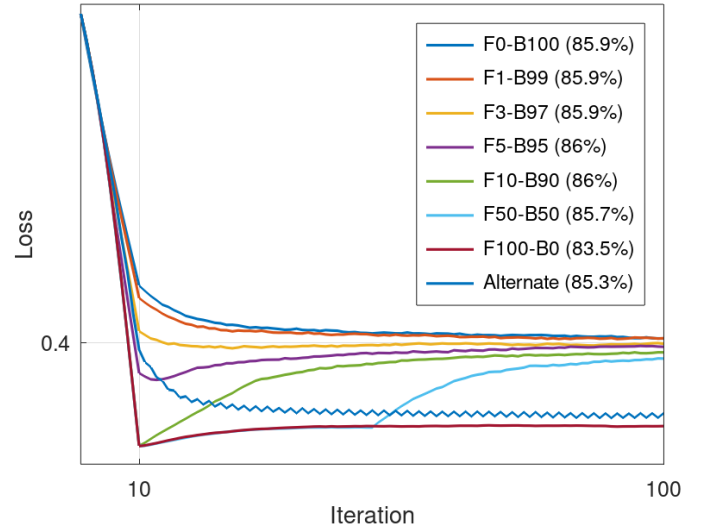


Fig. 8. Forward propagation (F) converges faster while backward propagation (B) alleviates overfitting. The numbers following F and B denote the number of learning steps T_{\rightarrow} and T_{\leftarrow} , respectively. The numbers in brackets represent robust accuracy against AutoAttack (Standard). “Alternate” represents the running of forward and backward propagation alternatively for 100 steps in total.

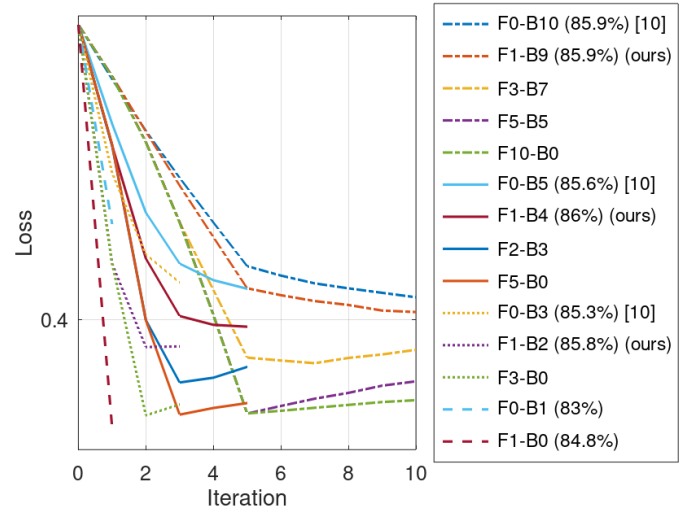


Fig. 9. By combining forward (F) and backward (B) propagation, Fast Preemption obtains performance comparable to that of the SOTA preemptive defense [10] by using only three steps (F1-B2). The numbers following F and B denote the number of learning steps T_{\rightarrow} and T_{\leftarrow} , respectively. The numbers in brackets represent robust accuracy against AutoAttack (Standard).

for preemptive defense, whereas using FGSM but without averaging leads to poor performance.

VIII. CONCLUSION

We have presented an efficient transferable preemptive adversarial defense that we call *Fast Preemption*. We demonstrated that with its framework and Fore-Back cascade learning algorithm, Fast Preemption offers transferable protection against adversarial attacks among unknown victim models without requiring ground truths. In terms of the time cost, clean accuracy, and robust accuracy, Fast Preemption outperformed benchmark training-time, test-time, and preemptive

TABLE VII
PERFORMANCE OF DIFFERENT BACKBONE MODELS.

| Backbone | Ablation | | | Time Cost (s) | White-box Defense | | | Transferable Defense | | |
|------------------------|-------------|-------------|----------------|---------------|-------------------|-------------|----------------|----------------------|-------------|----------------|
| | Clean (%) | PGD (%) | AutoAttack (%) | | Clean (%) | PGD (%) | AutoAttack (%) | Clean (%) | PGD (%) | AutoAttack (%) |
| Bi-Level [10] | 89.1 | 43.9 | 42.4 | 28 | 95.5 | 84.9 | 81.8 | 95.3 | 72.7 | 70.8 |
| RaWideResNet-70-16 [7] | 93.5 | 74.5 | 71.4 | 178 | 95.7 | 91.6 | 89.9 | 95.2 | 78.1 | 76.2 |
| PreActResNet-18 [5] | 88.1 | 61.8 | 58.6 | 26 | 93.8 | 85.9 | 83.3 | 95.4 | 79.6 | 77.3 |

To evaluate the performance of the backbone models in our framework, we followed the results from the previous section and used ResNeXt29-32x4d [37] as the classifier model, and 100 steps backward propagation as Bi-Level [10]. The transferable defenses were all evaluated using XCI-T-L12 [6] as the victim model, different from the backbone models.

TABLE VIII
PERFORMANCE FOR DIFFERENT N AND OPTIMIZATION ALGORITHMS.

| Optimization | Ablation N Samples | Time Cost (s) | Transferable Defense | | |
|--------------|-------------------------|---------------|----------------------|-------------|----------------|
| | | | Clean (%) | PGD (%) | AutoAttack (%) |
| PGD | 1 | 0.7 | 95.3 | 87.5 | 85.8 |
| FGSM | 1 | 0.04 | 95.4 | 86.8 | 85.4 |
| PGD | 20 | 0.8 | 95.2 | 87.7 | 85.9 |
| FGSM | 20 | 0.04 | 95.5 | 87.8 | 85.9 |

Forward propagation ran one step and backward propagation ran two steps. Transferable defense was evaluated using RaWideResNet-70-16 [7] as the victim model.

defenses. We also demonstrated that the protection from Fast Preemption is irreversible unless the backbone model, algorithm, and settings of the defense are all compromised.

This paper lays the theoretical foundation for a preemptive defense framework that can shape future research on each component's optimization instead of end-to-end application in the relevant field. The toolbox that will be released supports further development and offers a platform for discussing relevant technologies.

REFERENCES

- [1] I. J. Goodfellow, J. Shlens, and C. Szegedy, "Explaining and harnessing adversarial examples," *arXiv preprint arXiv:1412.6572*, 2014.
- [2] H. Wang, S. Wang, Z. Jin, Y. Wang, C. Chen, and M. Tistarelli, "Similarity-based gray-box adversarial attack against deep face recognition," in *2021 16th IEEE International Conference on Automatic Face and Gesture Recognition (FG 2021)*, pp. 1–8, 2021.
- [3] H. Wang, S. Wang, C. Chen, M. Tistarelli, and Z. Jin, "A multi-task adversarial attack against face authentication," *ACM Transactions on Multimedia Computing, Communications, and Applications*, may 2024.
- [4] K. Eykholt, I. Evtimov, E. Fernandes, B. Li, A. Rahmati, C. Xiao, A. Prakash, T. Kohno, and D. Song, "Robust physical-world attacks on deep learning visual classification," in *Proceedings of the IEEE conference on computer vision and pattern recognition (CVPR)*, pp. 1625–1634, 2018.
- [5] S. Goyal, S.-A. Rebuffi, O. Wiles, F. Stimberg, D. A. Calian, and T. A. Mann, "Improving robustness using generated data," *Advances in Neural Information Processing Systems (NeurIPS)*, vol. 34, pp. 4218–4233, 2021.
- [6] E. Debenedetti, V. Schwag, and P. Mittal, "A light recipe to train robust vision transformers," in *2023 IEEE Conference on Secure and Trustworthy Machine Learning (SaTML)*, pp. 225–253, 2023.
- [7] S. Peng, W. Xu, C. Cornelius, M. Hull, K. Li, R. Duggal, M. Phute, J. Martin, and D. H. Chau, "Robust principles: Architectural design principles for adversarially robust cnns," *arXiv preprint arXiv:2308.16258*, 2023.
- [8] C. Liu, Y. Dong, W. Xiang, X. Yang, H. Su, J. Zhu, Y. Chen, Y. He, H. Xue, and S. Zheng, "A comprehensive study on robustness of image classification models: Benchmarking and rethinking," *arXiv preprint arXiv:2302.14301*, 2023.
- [9] W. Nie, B. Guo, Y. Huang, C. Xiao, A. Vahdat, and A. Anandkumar, "Diffusion models for adversarial purification," in *International Conference on Machine Learning (ICML)*, pp. 16805–16827, 2022.
- [10] S. Moon, G. An, and H. O. Song, "Preemptive image robustification for protecting users against man-in-the-middle adversarial attacks," in *Proceedings of the AAAI Conference on Artificial Intelligence (AAAI)*, pp. 7823–7830, 2022.
- [11] I. Frosio and J. Kautz, "The best defense is a good offense: Adversarial augmentation against adversarial attacks," in *Proceedings of the IEEE/CVF Conference on Computer Vision and Pattern Recognition (CVPR)*, pp. 4067–4076, 2023.
- [12] M. Fredrikson, S. Jha, and T. Ristenpart, "Model inversion attacks that exploit confidence information and basic countermeasures," in *Proceedings of the 22nd ACM SIGSAC conference on computer and communications security (ACM CCS)*, pp. 1322–1333, 2015.
- [13] A. Saha, A. Subramanya, and H. Pirsiavash, "Hidden trigger backdoor attacks," in *Proceedings of the AAAI conference on artificial intelligence (AAAI)*, pp. 11957–11965, 2020.
- [14] N. D. Singh, F. Croce, and M. Hein, "Revisiting adversarial training for imagenet: Architectures, training and generalization across threat models," *arXiv preprint arXiv:2303.01870*, 2023.
- [15] A. Krizhevsky, G. Hinton, *et al.*, "Learning multiple layers of features from tiny images," tech. rep., University of Toronto, 2009.
- [16] I. G. Alex, K. Ben Hamner, "Nips 2017: Defense against adversarial attack," 2017.
- [17] A. Madry, A. Makelov, L. Schmidt, D. Tsipras, and A. Vladu, "Towards deep learning models resistant to adversarial attacks," in *International Conference on Learning Representations (ICLR)*, 2018.
- [18] F. Croce and M. Hein, "Reliable evaluation of adversarial robustness with an ensemble of diverse parameter-free attacks," in *International Conference on Machine Learning (ICML)*, pp. 2206–2216, 2020.
- [19] C. E. Shannon, "Communication theory of secrecy systems," *The Bell system technical journal*, vol. 28, no. 4, pp. 656–715, 1949.
- [20] A. Shafahi, M. Najibi, A. Ghiasi, Z. Xu, J. Dickerson, C. Studer, L. S. Davis, G. Taylor, and T. Goldstein, "Adversarial training for free!," in *Proceedings of the 33rd International Conference on Neural Information Processing Systems (NeurIPS)*, pp. 3358–3369, 2019.
- [21] V. Schwag, S. Mahloujifar, T. Handina, S. Dai, C. Xiang, M. Chiang, and P. Mittal, "Robust learning meets generative models: Can proxy distributions improve adversarial robustness?," in *International Conference on Learning Representations (ICLR)*, 2021.
- [22] J. Ho, A. Jain, and P. Abbeel, "Denosing diffusion probabilistic models," in *Proceedings of the 34th International Conference on Neural Information Processing Systems (NeurIPS)*, pp. 6840–6851, 2020.
- [23] Z. Wang, T. Pang, C. Du, M. Lin, W. Liu, and S. Yan, "Better diffusion models further improve adversarial training," *arXiv preprint arXiv:2302.04638*, 2023.
- [24] T. Karras, M. Aittala, T. Aila, and S. Laine, "Elucidating the design space of diffusion-based generative models," *Advances in Neural Information Processing Systems (NeurIPS)*, vol. 35, pp. 26565–26577, 2022.
- [25] J. Dong, S.-M. Moosavi-Dezfooli, J. Lai, and X. Xie, "The enemy of my enemy is my friend: Exploring inverse adversaries for improving adversarial training," in *Proceedings of the IEEE/CVF Conference on Computer Vision and Pattern Recognition (CVPR)*, pp. 24678–24687, 2023.
- [26] G. Cohen, G. Sapiro, and R. Giryes, "Detecting adversarial samples using influence functions and nearest neighbors," in *Proceedings of the IEEE/CVF Conference on Computer Vision and Pattern Recognition (CVPR)*, pp. 14453–14462, 2020.
- [27] F. Zuo and Q. Zeng, "Exploiting the sensitivity of 12 adversarial examples to erase-and-restore," in *Proceedings of the 2021 ACM Asia Conference on Computer and Communications Security (ACM Asia CCS)*, p. 40–51, 2021.
- [28] B. Liang, H. Li, M. Su, X. Li, W. Shi, and X. Wang, "Detecting adversarial image examples in deep neural networks with adaptive noise

reduction,” *IEEE Transactions on Dependable and Secure Computing*, vol. 18, no. 1, pp. 72–85, 2021.

- [29] T. Hickling, N. Aouf, and P. Spencer, “Robust adversarial attacks detection based on explainable deep reinforcement learning for uav guidance and planning,” *IEEE Transactions on Intelligent Vehicles*, 2023.
- [30] Q. Wang, W. Guo, K. Zhang, A. G. Ororbia, X. Xing, X. Liu, and C. L. Giles, “Adversary resistant deep neural networks with an application to malware detection,” in *Proceedings of the 23rd ACM SIGKDD International Conference on Knowledge Discovery and Data Mining (ACM SIGKDD)*, pp. 1145–1153, 2017.
- [31] C. Guo, M. Rana, M. Cisse, and L. van der Maaten, “Countering adversarial images using input transformations,” in *International Conference on Learning Representations (ICLR)*, 2018.
- [32] E. Raff, J. Sylvestre, S. Forsyth, and M. McLean, “Barrage of random transforms for adversarially robust defense,” in *Proceedings of the IEEE/CVF Conference on Computer Vision and Pattern Recognition (CVPR)*, pp. 6528–6537, 2019.
- [33] M. Ren, Y. Zhu, Y. Wang, and Z. Sun, “Perturbation inactivation based adversarial defense for face recognition,” *IEEE Transactions on Information Forensics and Security*, vol. 17, pp. 2947–2962, 2022.
- [34] D. P. Kingma and M. Welling, “Auto-encoding variational bayes,” in *International Conference on Learning Representations (ICLR)*, 2014.
- [35] M. Alfara, J. C. Pérez, A. Thabet, A. Bibi, P. H. Torr, and B. Ghanem, “Combating adversaries with anti-adversaries,” in *Proceedings of the AAAI Conference on Artificial Intelligence (AAAI)*, vol. 36(6), pp. 5992–6000, 2022.
- [36] H. Salman, A. Ilyas, L. Engstrom, S. Vemprala, A. Madry, and A. Kapoor, “Unadversarial examples: Designing objects for robust vision,” *Advances in Neural Information Processing Systems (NeurIPS)*, vol. 34, pp. 15270–15284, 2021.
- [37] D. Hendrycks, N. Mu, E. D. Cubuk, B. Zoph, J. Gilmer, and B. Lakshminarayanan, “Augmix: A simple data processing method to improve robustness and uncertainty,” in *International Conference on Learning Representations (ICLR)*, 2019.
- [38] R. Tian, Z. Wu, Q. Dai, H. Hu, and Y.-G. Jiang, “Deeper insights into the robustness of vits towards common corruptions,” *arXiv preprint arXiv:2204.12143*, 2022.
- [39] F. Croce and M. Hein, “Minimally distorted adversarial examples with a fast adaptive boundary attack,” in *International Conference on Machine Learning (ICML)*, pp. 2196–2205, 2020.
- [40] M. Andriushchenko, F. Croce, N. Flammarion, and M. Hein, “Square attack: a query-efficient black-box adversarial attack via random search,” in *European Conference on Computer Vision (ECCV)*, pp. 484–501, 2020.
- [41] A. Athalye, N. Carlini, and D. Wagner, “Obfuscated gradients give a false sense of security: Circumventing defenses to adversarial examples,” in *International Conference on Machine Learning (ICML)*, pp. 274–283, 2018.
- [42] Z. Wang, A. C. Bovik, H. R. Sheikh, and E. P. Simoncelli, “Image quality assessment: from error visibility to structural similarity,” *IEEE Transactions on Image Processing*, vol. 13, no. 4, pp. 600–612, 2004.
- [43] M.-I. Nicolae, M. Sinn, M. N. Tran, B. Buesser, A. Rawat, M. Wistuba, V. Zantedeschi, N. Baracaldo, B. Chen, H. Ludwig, I. Molloy, and B. Edwards, “Adversarial robustness toolbox v1.2.0,” *CoRR*, 2018.
- [44] F. Croce, M. Andriushchenko, V. Sehwag, E. Debenedetti, N. Flammarion, M. Chiang, P. Mittal, and M. Hein, “Robustbench: a standardized adversarial robustness benchmark,” in *Thirty-fifth Conference on Neural Information Processing Systems Datasets and Benchmarks Track (Round 2) (NeurIPS 2021)*, 2021.
- [45] D. Livingston, “Colorimetric analysis of the ntsc color television system,” *Proceedings of the IRE*, vol. 42, no. 1, pp. 138–150, 1954.



Hanrui Wang received his B.S. degree in Electronic Information Engineering from Northeastern University (China) in 2011. He left the IT industry from a director position in 2019 to pursue a research career and received his Ph.D. in Computer Science from Monash University, Australia, in January 2024. He is currently working as a Postdoctoral Researcher with the Echizen Laboratory at the National Institute of Informatics (NII) in Tokyo, Japan. His research interests include AI security and privacy, particularly adversarial machine learning.



Ching-Chun Chang received his PhD in Computer Science from the University of Warwick, UK, in 2019. He participated in a short-term scientific mission supported by European Cooperation in Science and Technology Actions at the Faculty of Computer Science, Otto-von-Guericke-Universität Magdeburg, Germany, in 2016. He was granted the Marie-Curie fellowship and participated in a research and innovation staff exchange scheme supported by Marie Skłodowska-Curie Actions at the Department of Electrical and Computer Engineering, New Jersey Institute of Technology, USA, in 2017. He was a Visiting Scholar with the School of Computer and Mathematics, Charles Sturt University, Australia, in 2018, and with the School of Information Technology, Deakin University, Australia, in 2019. He was a Research Fellow with the Department of Electronic Engineering, Tsinghua University, China, in 2020. He is currently a Postdoctoral Research Fellow with the National Institute of Informatics, Japan. His research interests include artificial intelligence, biometrics, communications, computer vision, cryptography, cybernetics, cybersecurity, evolutionary computation, forensics, information theory, linguistics, mathematical optimization, natural language processing, privacy engineering, psychology, signal processing, steganography, time series forecasting, and watermarking, within the scope of computer science.



Chun-Shien Lu received the Ph.D. degree in Electrical Engineering from National Cheng-Kung University, Tainan, Taiwan in 1998. He is a full research fellow (full professor) in the Institute of Information Science since March 2013 and the executive director in the Taiwan Information Security Center, Research Center for Information Technology Innovation, Academia Sinica, Taipei, Taiwan, since June 2024. His current research interests mainly focus on deep learning, AI security and privacy, and inverse problems. Dr. Lu serves as a Technical

Committee member of Communications and Information Systems Security (CIS-TC) and Multimedia Communications Technical Committee (MMTC), IEEE Communications Society, since 2012 and 2017, respectively. Dr. Lu also serves as Area Chairs of ICASSP 2012 2014, ICIP 2019-2024, ICML 2020, ICML 2023 2024, ICLR 2021 2024, NeurIPS 2022 2024, and ACM Multimedia 2022 2024. Dr. Lu has owned four US patents, five ROC patents, and one Canadian patent in digital watermarking and graphic QR code. Dr. Lu won Ta-You Wu Memorial Award, National Science Council in 2007 and was a co-recipient of a National Invention and Creation Award in 2004. Dr. Lu was an associate editor of *IEEE Trans. on Image Processing* from 2010/12 to 2014 and from 2018/3 to 2023/6.



Isao Echizen (Senior Member, IEEE) received B.S., M.S., and D.E. degrees from the Tokyo Institute of Technology, Japan, in 1995, 1997, and 2003, respectively. He joined Hitachi, Ltd. in 1997 and until 2007 was a research engineer in the company's systems development laboratory. He is currently a director and a professor of the Information and Society Research Division, the National Institute of Informatics (NII), a director of the Global Research Center for Synthetic Media, the NII, a professor in the Department of Information and Communication

Engineering, Graduate School of Information Science and Technology, the University of Tokyo, and a professor in the Graduate Institute for Advanced Studies, the Graduate University for Advanced Studies (SOKENDAI), Japan. He was a visiting professor at the University of Freiburg, Germany, and at the University of Halle-Wittenberg, Germany. He is currently engaged in research on multimedia security and multimedia forensics. He is a research director in the CREST FakeMedia project, Japan Science and Technology Agency (JST). He received the Best Paper Award from the IEICE in 2023, the Best Paper Awards from the IPSJ in 2005 and 2014, the IPSJ Nagao Special Researcher Award in 2011, the DOCOMO Mobile Science Award in 2014, the Information Security Cultural Award in 2016, and the IEEE Workshop on Information Forensics and Security Best Paper Award in 2017. He was a member of the Information Forensics and Security Technical Committee of the IEEE Signal Processing Society. He is the IEICE Fellow, the IPSJ fellow, the IEEE Senior Member, and the Japanese representative on IFIP TC11 (Security and Privacy Protection in Information Processing Systems), a member-at-large of the board-of-governors of APSIPA, and an editorial board member of the IEEE Transactions on Dependable and Secure Computing, the EURASIP Journal on Image and Video processing, and the Journal of Information Security and Applications, Elsevier.